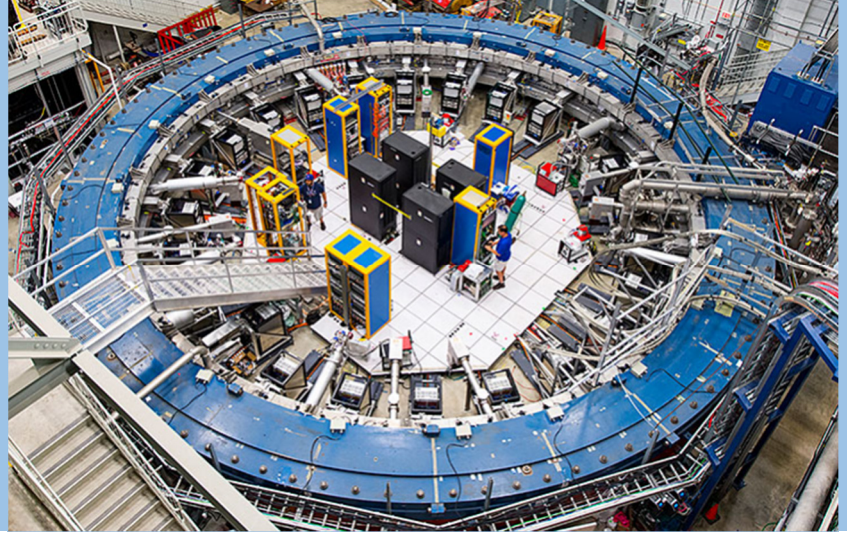

The Accelerator and Beam Physics of the Muon *g-2* Experiment at Fermilab

David A. Tarazona

IPAC22

June 13, 2022

Muon *g-2* Experiment at Fermilab, First Results from “Run-1”

On April 7th, 2021, we (E989) released the first (Run-1) results of the Muon *g-2* Experiment at Fermilab:

$$a_\mu(\text{FNAL, Run 1}) = 116592040(54) \times 10^{-11} \ (0.46 \text{ ppm})$$

Muon *g-2* Experiment at Fermilab, First Results from "Run-1"

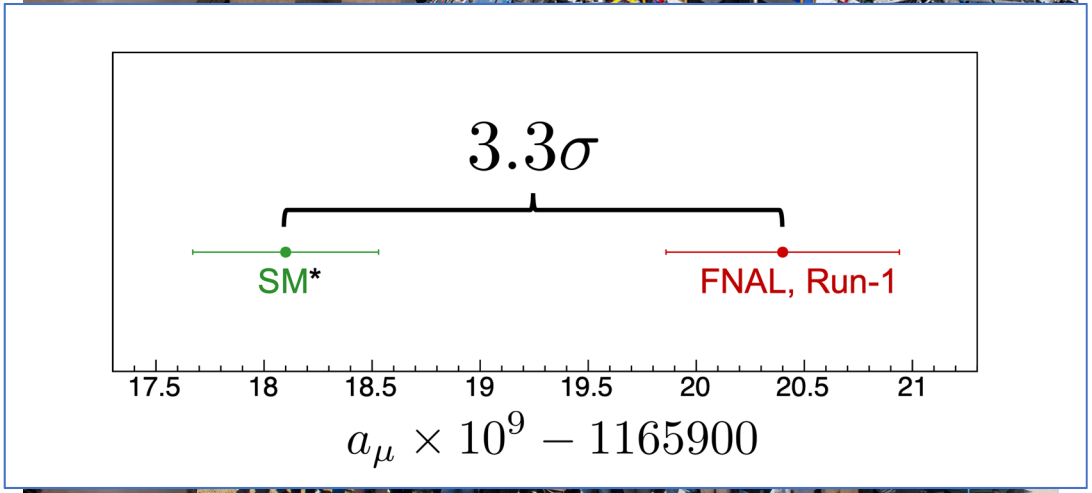

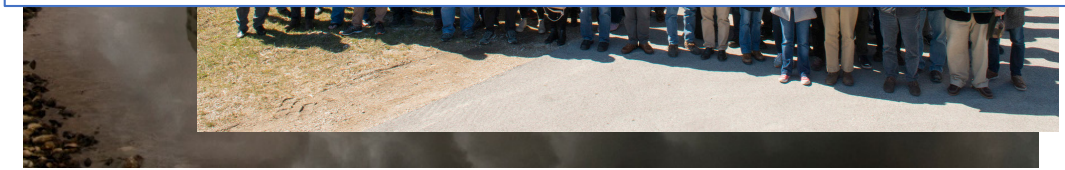

On April 7th, 2021, we (E989) released the first (Run-1) results of the Muon *g-2* Experiment at Fermilab:

$$a_\mu(\text{FNAL, Run 1}) = 116592040(54) \times 10^{-11} \ (0.46 \text{ ppm})$$

This talk is about:

1. What is "*g*-2" of a muon?
2. Storage ring: purpose and parameters.
3. Magnetic field.
4. Muon beam production/injection/confinement.
5. Beam dynamics corrections.

*From Muon g-2 Theory Initiative: Phys. Rep. **887**, 1 (2020).

What is "*g-2*" of a muon? a_μ from SM

$$\boldsymbol{m} = g\frac{e}{2m_\mu}\boldsymbol{s}$$

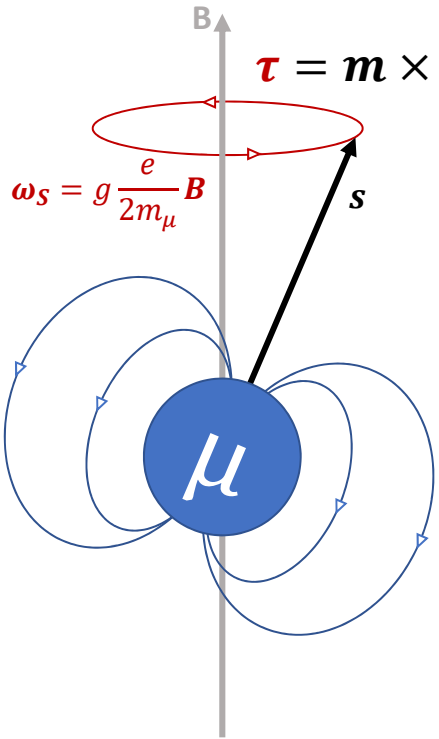

- In 1928, Dirac equation (relativistic QM) predicted

$$g = 2.$$

- By April 2021, the Standard Model predicts (for muons)*

$$g = 2.0023318362(86),$$

or

$$a_\mu^{SM} \equiv \frac{(g-2)}{2} = 0.00116591810(43)$$

*From Muon g-2 Theory Initiative: Phys. Rep. **887**, 1 (2020).

What is "*g-2*" of a muon? a_μ from SM

$$\boldsymbol{m} = g\frac{e}{2m_\mu}\boldsymbol{s}$$

$$\boldsymbol{\tau} = \boldsymbol{m} \times \boldsymbol{B}$$

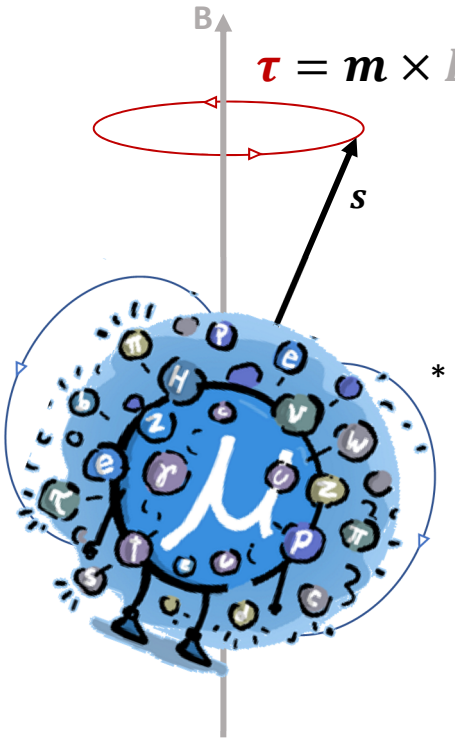

- The Standard Model encompasses all known contributions to a_μ from quantum fluctuations in the form of intermediate elementary particles, i.e., radiative corrections.

$$a_\mu^{SM} \equiv \frac{g\text{-}2}{2} = 0.00116591810(43)$$

*Cartoon from Dr. Cham (https://physics.aps.org/articles/v14/47).

What is "*g-2*" of a muon? a_μ from SM

Standard Model

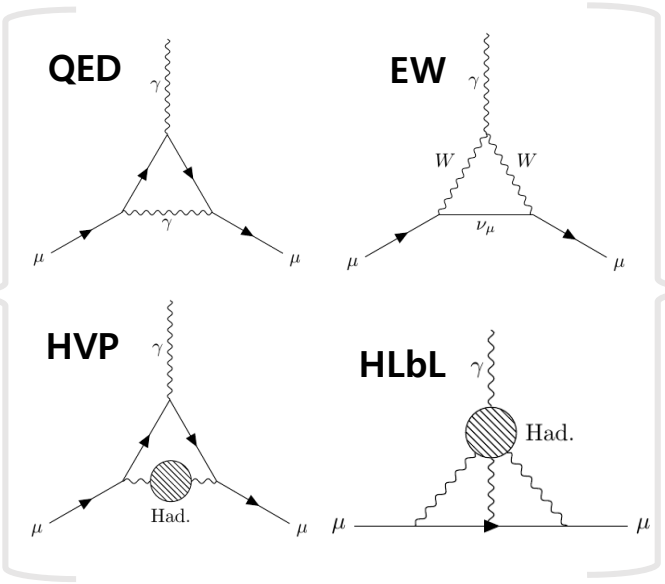

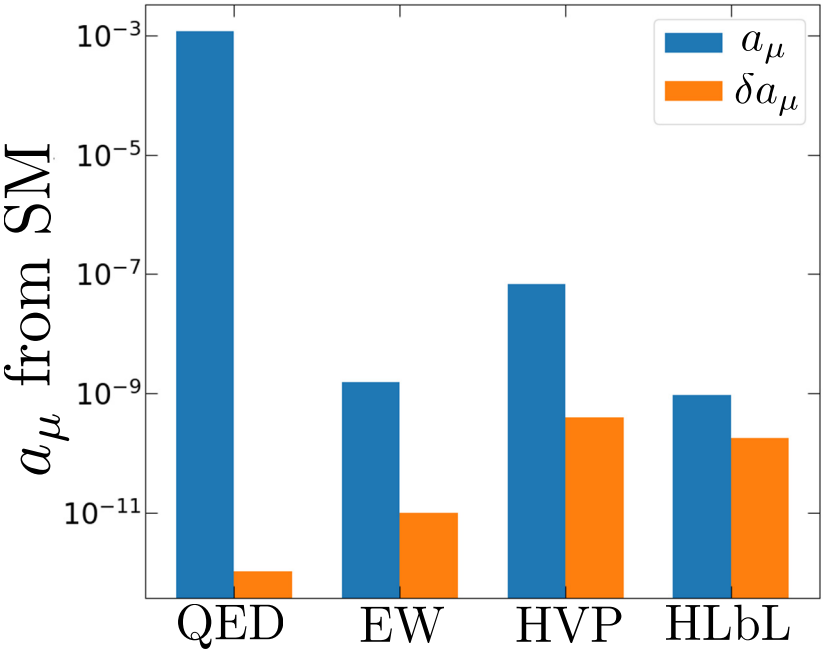

$$a_\mu^{\mathrm{SM}} = a_\mu^{\mathrm{QED}} + a_\mu^{\mathrm{Weak}} + a_\mu^{\mathrm{HVP}} + a_\mu^{\mathrm{HLbL}} = 116591810\,(43) \times 10^{-11}$$

*From Muon g-2 Theory Initiative: Phys. Rep. **887**, 1 (2020).

Purpose of the Muon *g-2* Storage Ring

e: Higher-energy positrons

- Purpose: To provide ~3GeV positrons out of muon beam decay for calorimetry.

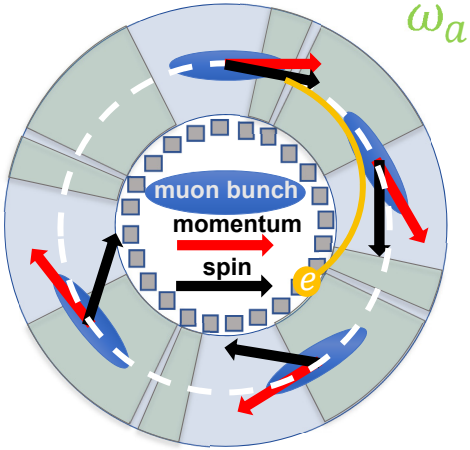

$$\omega_a = \omega_S - \omega_C = -\frac{e}{m} a_\mu \langle B \rangle$$

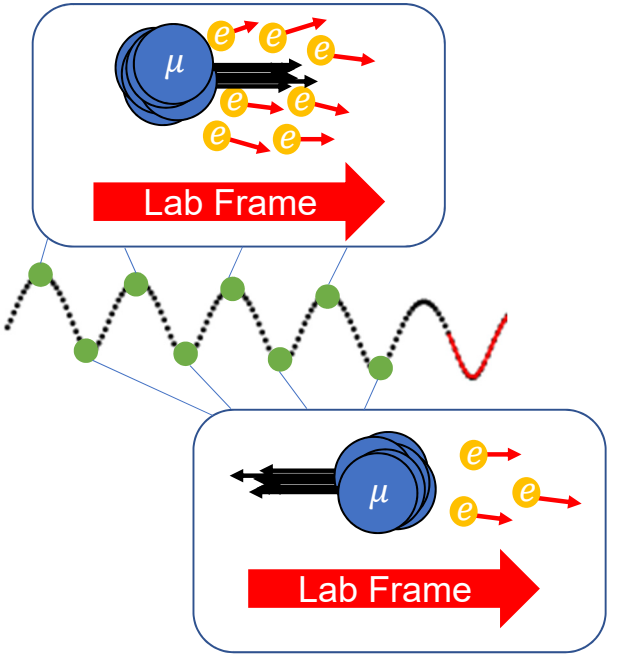

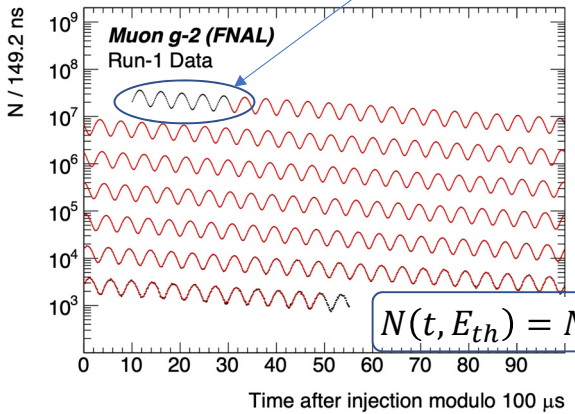

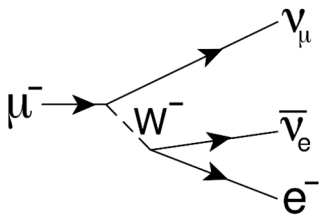

ω_a: Spin precession frequency relative to the momentum direction of muons in the of the storage ring

$$N(t, E_{th}) = N_0(E_{th}) \exp^{-t/\gamma\tau_\mu} [1 + A(E_{\rm th}) \cos(\omega_a t + \varphi_0(E_{th}))]$$

Purpose of the Muon *g-2* Storage Ring

e: Higher-energy positrons

- Purpose: To provide ~3GeV positrons out of muon beam decay for calorimetry.

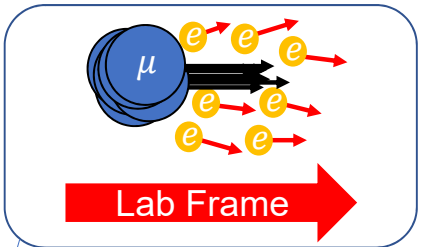

$$\omega_a = \omega_S - \omega_C = -\frac{e}{m} a_\mu \langle B \rangle$$

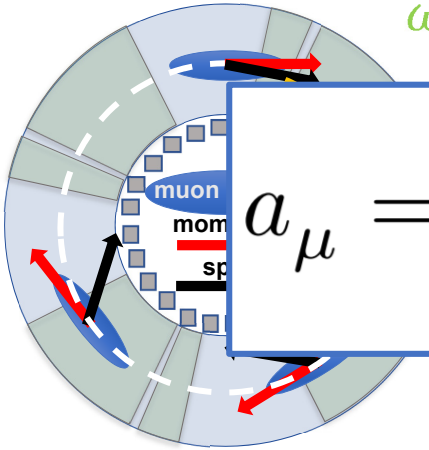

$$a_\mu = \frac{\omega_a}{\tilde{\omega}'_p(T_r)} \frac{\mu'_p(T_r)}{\mu_e(H)} \frac{\mu_e(H)}{\mu_e} \frac{m_\mu}{m_e} \frac{g_e}{2}$$

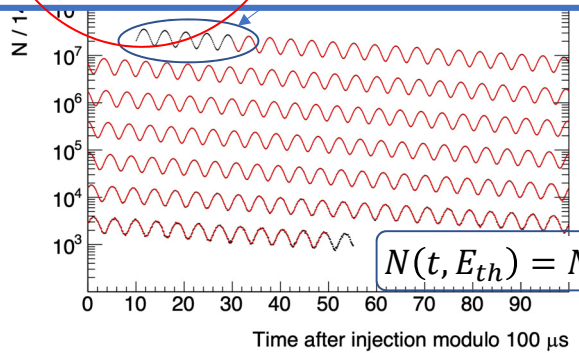

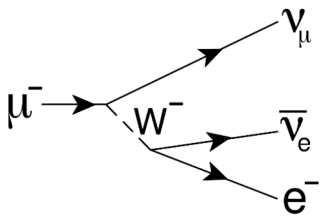

ω_a: Spin precession frequency relative to the momentum direction of muons in the of the storage ring

$$N(t, E_{th}) = N_0(E_{th}) \exp^{-t/\gamma\tau_\mu} [1 + A(E_{\rm th}) \cos(\omega_a t + \varphi_0(E_{th}))]$$

Purpose of the Muon *g-2* Storage Ring

- The ring is designed to allow a highly precise measurement of the muon anomalous magnetic moment anomaly $a_\mu \equiv (g_\mu - 2)/2$ ($\Delta a_\mu / a_\mu \leq 140$ ppb):

$$a_\mu = \frac{\omega_a}{\tilde{\omega}'_p(T_r)} \frac{\mu'_p(T_r)}{\mu_e(H)} \frac{\mu_e(H)}{\mu_e} \frac{m_\mu}{m_e} \frac{g_e}{2}$$

Main measurements:

- ω_a: The "anomalous precession frequency"

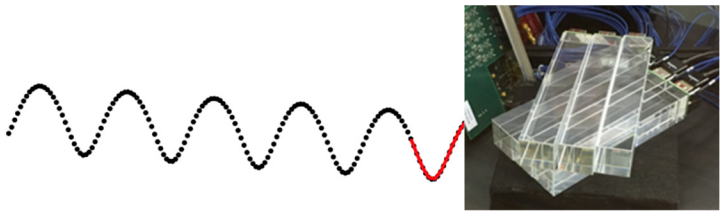

- $\tilde{\omega}'_p$: Proton Larmor frequency measured in a spherical water sample, weighted by the muon distribution $\left(B = \frac{\hbar \omega_p}{2\mu_p}\right)$.

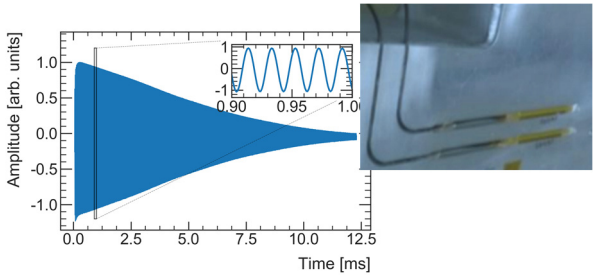

Ring and optical lattice parameters

Parameter	Value
Nominal momentum (p_0)	3.094 GeV/c
Momentum acceptance	±0.56%
Radial tune (ν_x)	0.944
Vertical tune (ν_y)	0.330
Bending magnetic field (B_0)	1.4513 T
Bending radius (ρ_0)	7.112 m
Revolution period	149.2 ns
Horizontal admittance	268π mm.mrad
Vertical admittance	93π mm.mrad
Maximum excursion	45 mm
x' max	6 mrad
y' max	2 mrad
High-voltage (HV) setpoint	$\sim$ ±18.3 kV
Vacuum in storage volume	$\lesssim 10^{-6}$ Torr
Current	5170 A

*Representative values

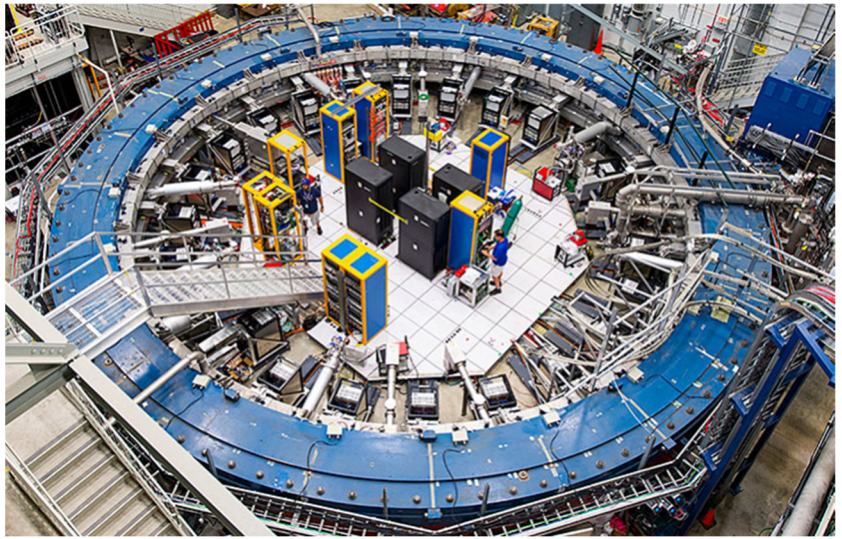

Parameter	Value (~)	Azimuthal Variation
α_x	0	$< \pm 0.1$
β_x	7.5 m	< 3%
γ_x	0.13 m^{-1}	< 3%
D_x	8 m	< 2%
α_y	0	$< \pm 0.2$
β_y	21.5 m	< 3%
γ_y	0.046 m^{-1}	< 1%
D_y	0.03 m	$< \pm 0.01$ m

*Representative values

- Temporal stability and spatial homogeneity of the magnetic guide field are essential to the experiment.
- Average magnetic field experienced by stored muons needs to remain stable on the scale of ppm.

Magnetic field measurement (i.e., $\tilde{\omega}'_p$)

$$\tilde{B} = \frac{\hbar\tilde{\omega}'_p(T)}{2\mu'_p(T)} = \frac{\hbar\tilde{\omega}'_p(T)}{2}\underbrace{\frac{\mu_e(H)}{\mu'_p(T)}\frac{\mu_e}{\mu_e(H)}\frac{1}{\mu_e}}$$

Known to ~10 ppb precision

$$\tilde{\omega}'_p(T_r) = \underbrace{f_{\mathrm{calib}}}\ \underbrace{\langle\omega_p(x,y,\phi)}\times\underbrace{M(x,y,\phi)\rangle}\,(1+\underbrace{B_k}+\underbrace{B_q})$$

- f_{calib}: NMR probe calibration factor
- $\langle\omega_p(x,y,\phi)$: Larmor frequency from proton NMR
- $M(x,y,\phi)\rangle$: Muon beam distribution
- B_k: Correction from beam injection system
- B_q: Correction from beam focusing system

Main magnet

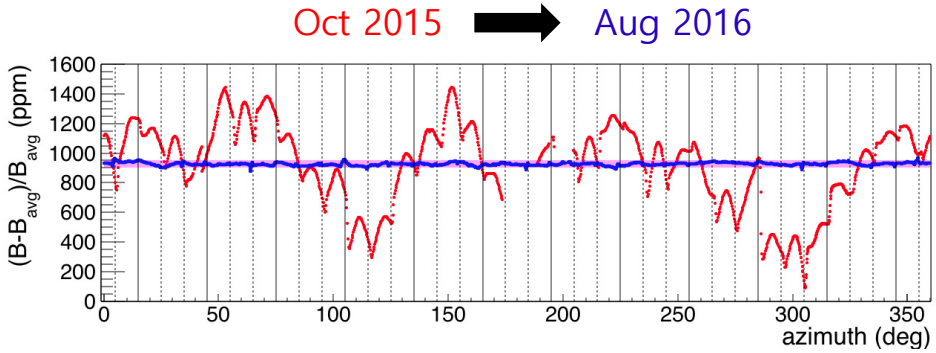

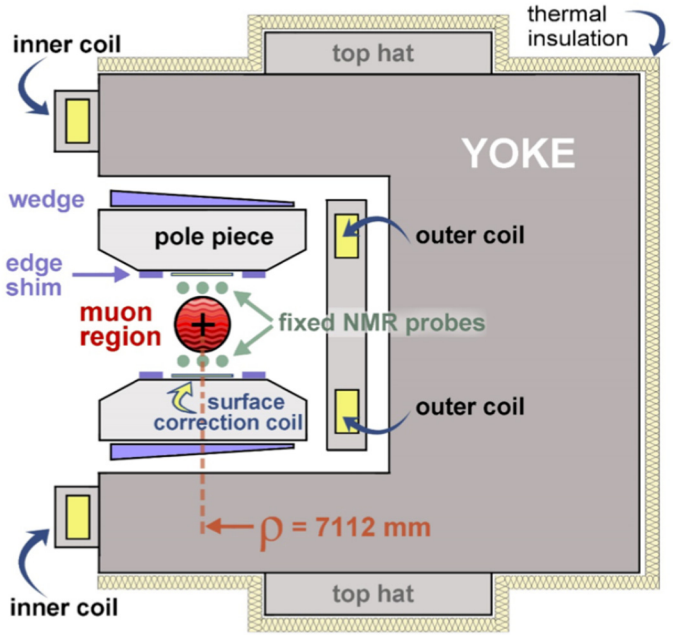

- Magnet shimming keeps the field highly uniform (local variations <50 ppm).
  - Passive shimming:
    - *Pole pieces positioning* drives the overall field strength.
    - *Additional pieces of iron* fine-tune azimuthally averaged field and control transverse gradients.
  - Active shimming:
    - *Surface coils* target specific azimuthally averaged multipoles.
    - *Power supply feedback* adjusts supply current to keep the average vertical field constant over time.

Magnetic field measurement

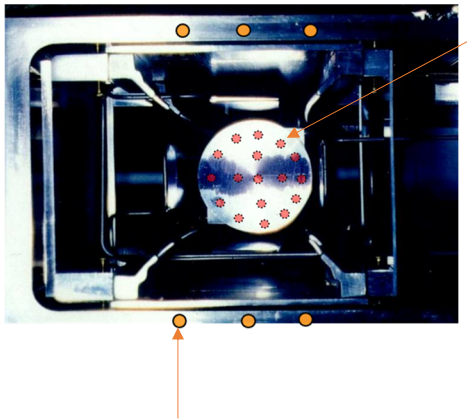

Field tracking between trolley runs is continuously tracked by 378 fixed NMR probes located throughout the ring.

Field in storage region mapped out by mobile NMR trolley every ~1-3 days.

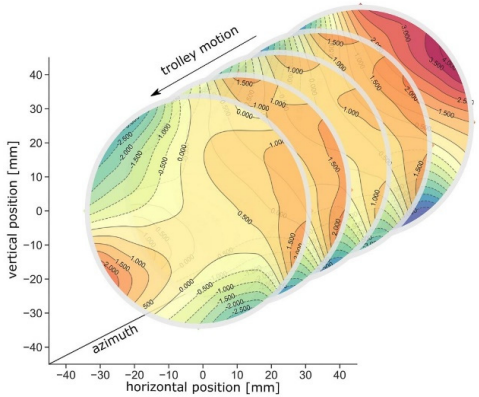

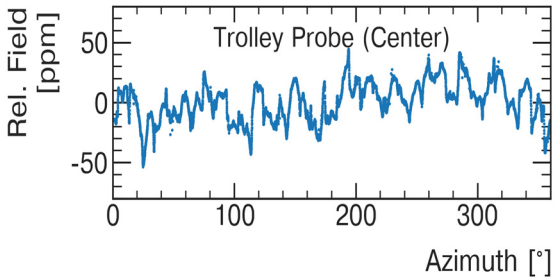

- Systematic effects associated with field mapping:
  - Position uncertainties (~5-25 ppb*)
  - Motion effects (~5-25 ppb)
  - Temperature effects (~5-25 ppb)
  - Configurations (<22 ppb)

- Systematic effects associated with field tracking, from tracking offsets for all fixed probe stations (~20-40 ppb).

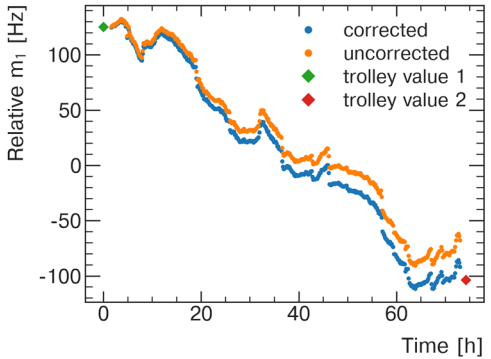

*Systematic errors representative of Run-1.

Magnetic field, beam-weighted

- 2D mapping of the field is described as a multipole expansion:

$$B \approx B_y = A_0 + \sum_{n=1}^{4} \left(\frac{r}{r_0}\right)^n (A_n \cos(n\theta) + B_n \sin(n\theta))$$

- Local variations of radial and azimuthal fields (typically <100 ppm of main field) lead to $(B - B_y)/B = O(10\ \text{ppb})$.

- The weighting simplifies to combining normal/skew terms in field expansion (c_n, s_n) with beam's multipole normal/skew projections (I_n, J_n) along azimuth:

$$\tilde{B} = c_0 + \sum_{n=1}^{4} (c_n I_n + s_n J_n)$$

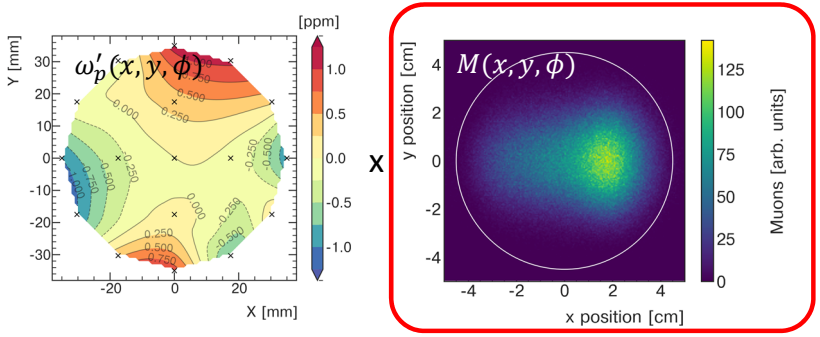

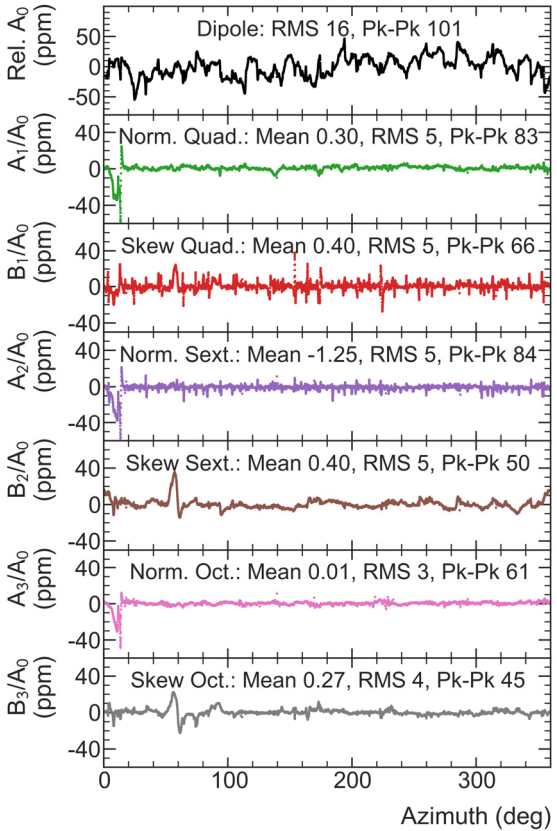

Muon beam injection

- **Injection** kickers aim to align muons with storage region.

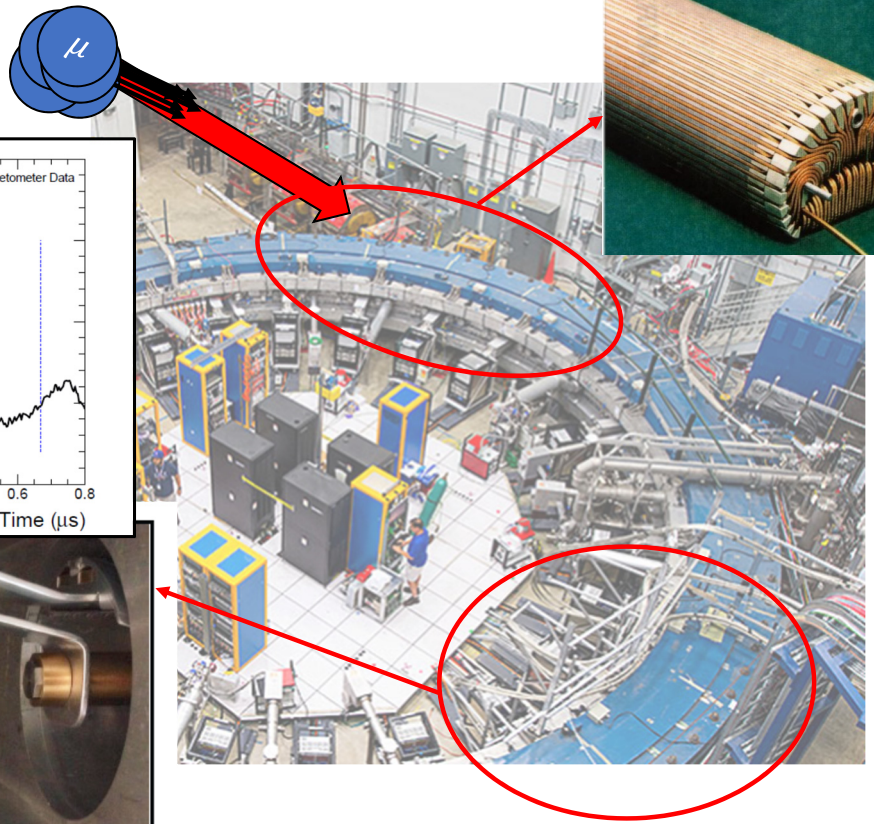

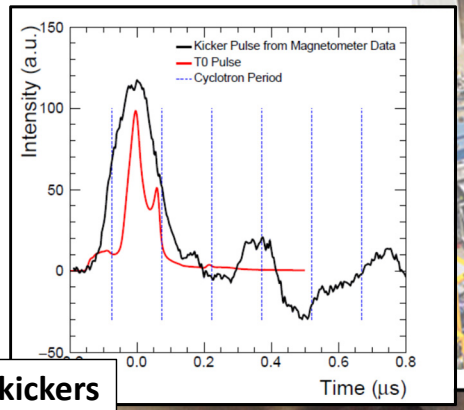

Injection kickers

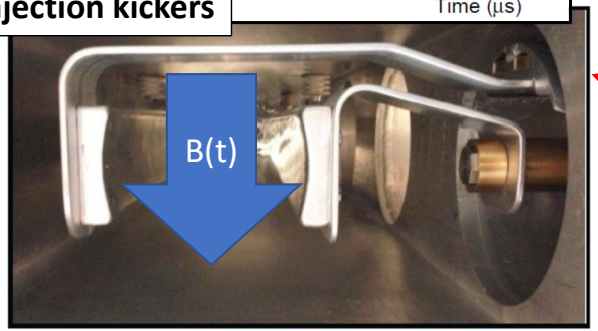

Inflector magnet

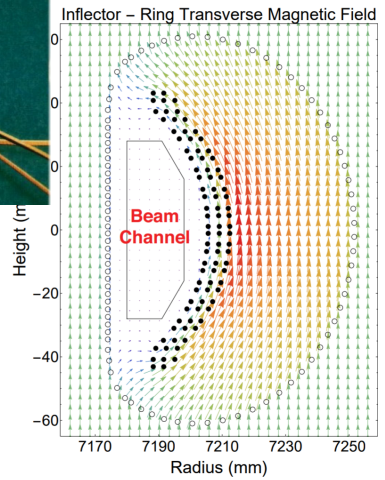

- **Inflector magnet** cancels the main focusing magnetic field (1.5 T) to inject the bunch directly.

Muon beam injection

- **Injection** kickers aim to align muons with storage region.

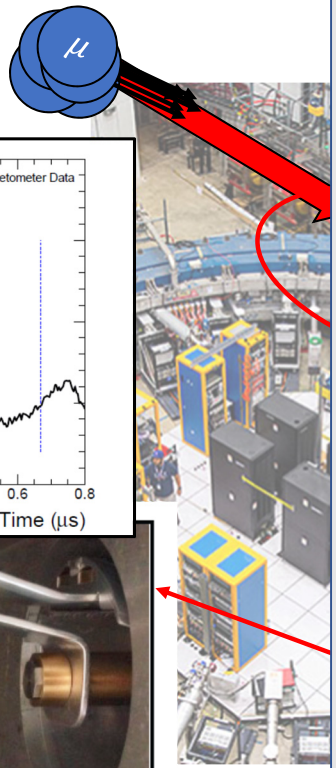

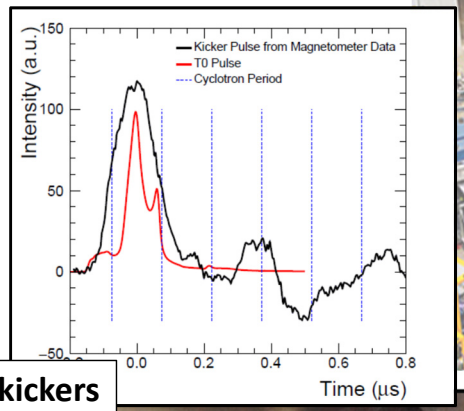

Injection kickers

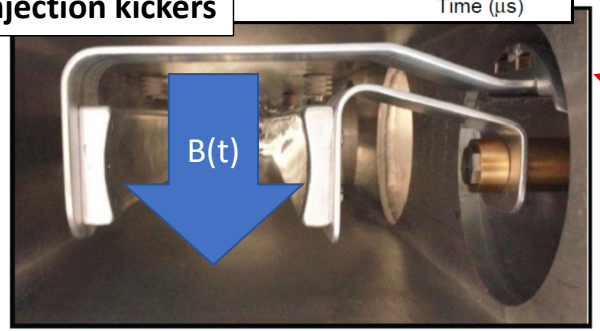

Kicker transient field

- Fast kicker pulses impedance mismatch induces eddy currents.

- Faraday magnetometer using fibers measured the kicker transient field (laser polarization rotates in TGG crystal in presence of the magnetic field).

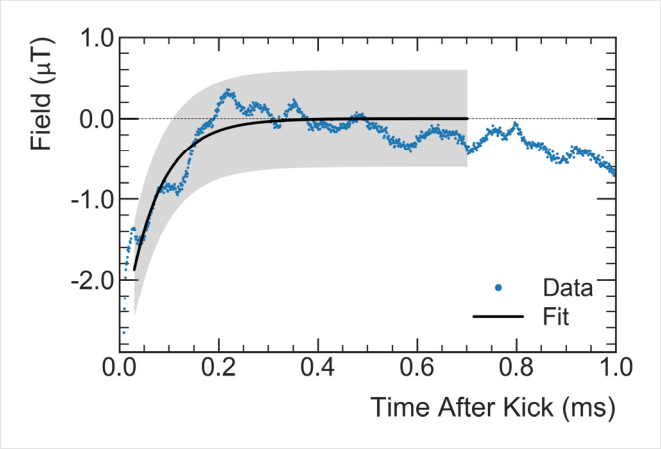

$B_k = -27(37)$ ppb for Run-1

Muon beam injection

- Imperfect injection kick creates beam's radial centroid oscillation (aka "Coherent Betatron Oscillation" CBO).

$$f_{CBO} = f_C(1 - \nu_x) \approx 0.37 \text{ MHz}$$

- Optics mismatch between injected beam and ring produces beam's radial width oscillation.

- Beam's transverse profile is measured with gaseous straw tracking detector:

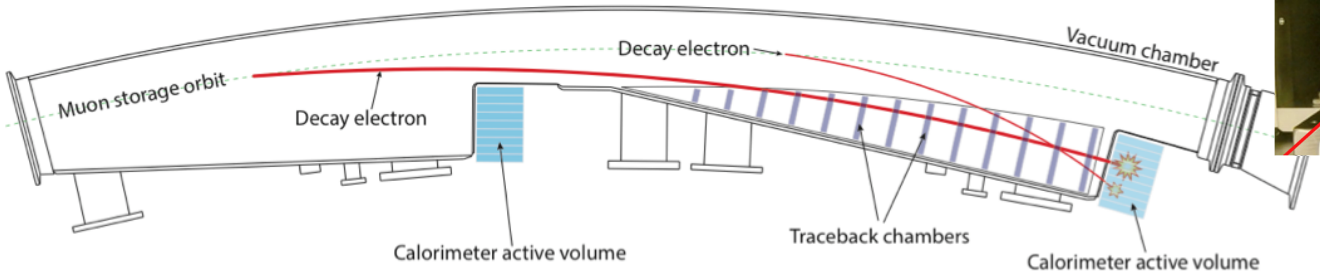

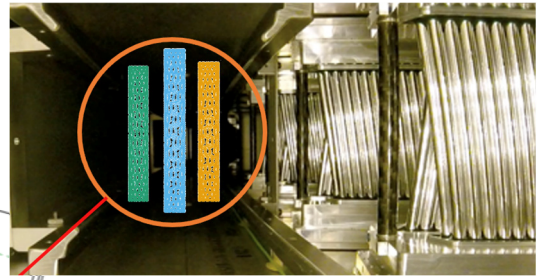

Muon beam vertical confinement

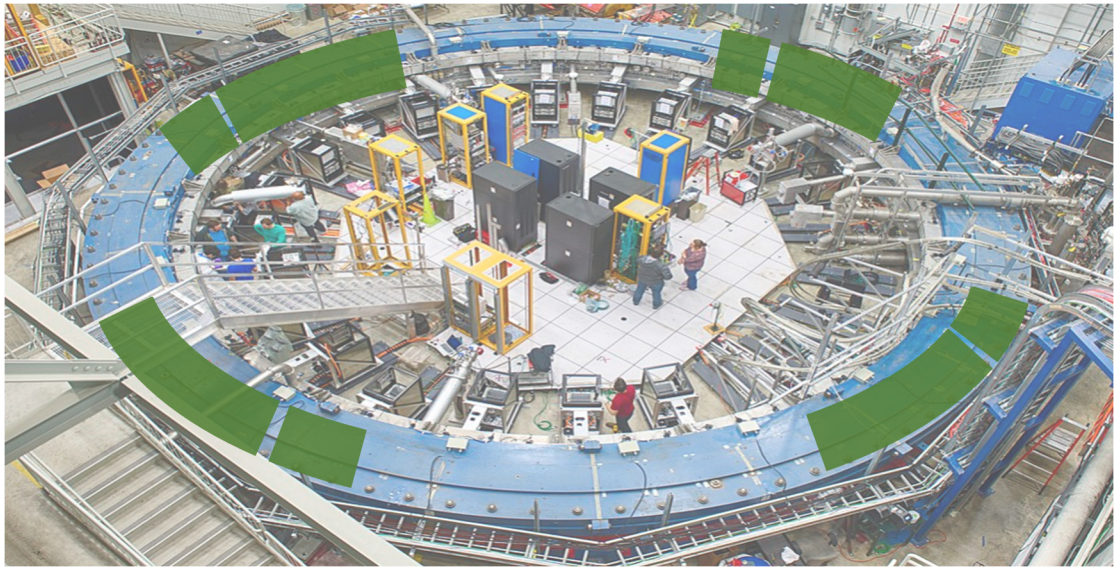

Muon beam vertical confinement

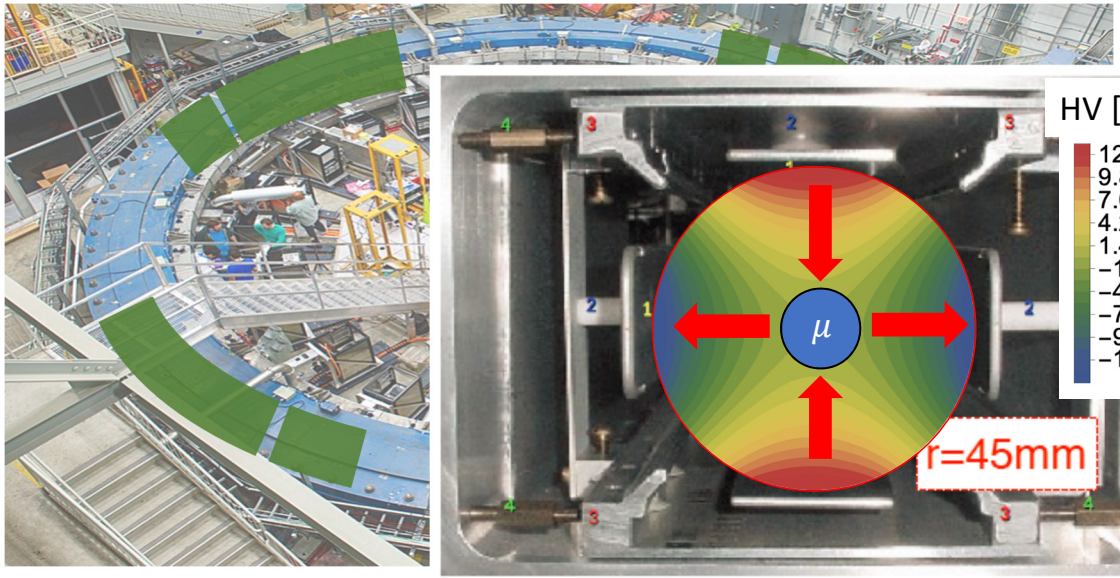

Quad plates mechanical vibration

- The ESQ plates are pulsed at 100 Hz.
- Mechanical vibrations induce a magnetic field transient in the storage region.

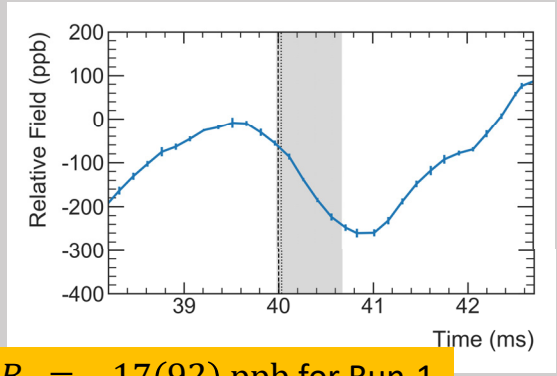

$B_q = -17(92)$ ppb for Run-1

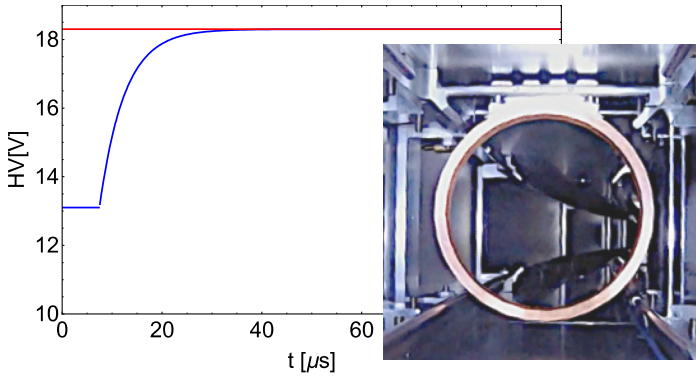

- The ElectroStatic Quadrupole system (ESQ) provides vertical focusing.
- The ESQ plates are mis-powered for closed orbit distortions.
- New application of radio-frequency (RF) electric fields minimizes CBO.

Optical lattice

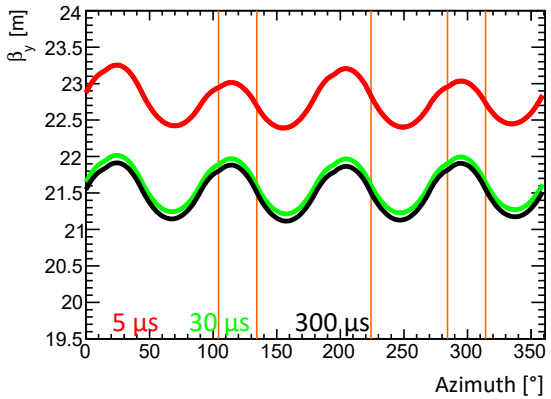

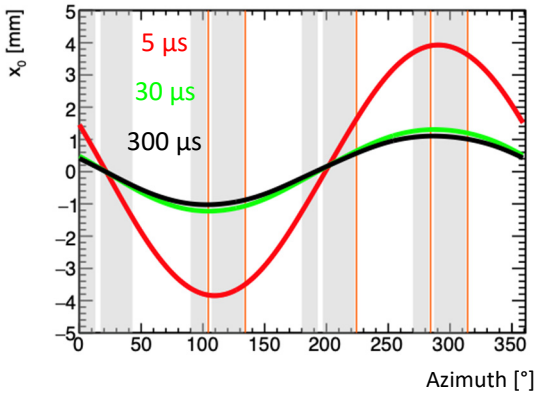

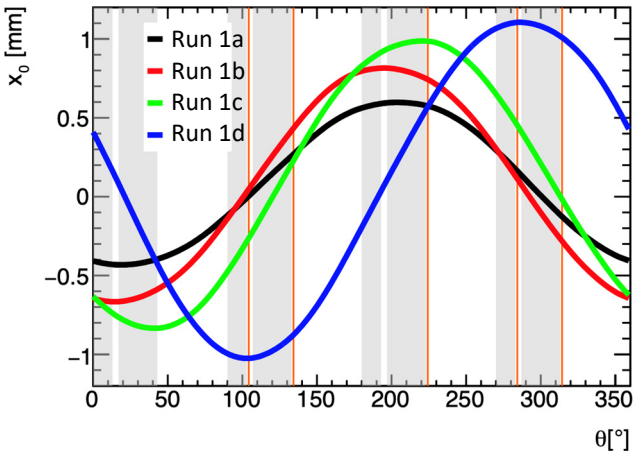

- Beam stability is provided by relatively weak focusing:

$$x'' + \frac{1-n}{\rho_0^2}x = 0$$
$$y'' + \frac{n}{\rho_0^2}y = 0$$

- Field index *n* from ESQ system:

$$n = \frac{\rho_0}{vB_0}\frac{\partial E_y}{\partial y}$$

$$n \approx 0.1 \quad , \quad 0 \le n \le 1$$

- Weak-focusing modelling provides 1st order ring representation:

$$\beta_x(s) \approx \frac{\rho_0}{\sqrt{1-n}} \qquad \beta_y(s) \approx \frac{\rho_0}{\sqrt{n}} \qquad D_x(s) \approx \frac{\rho_0}{1-n}$$

$$Q_y \approx \sqrt{n} \qquad Q_x \approx \sqrt{1-n}$$

Nonlinearities

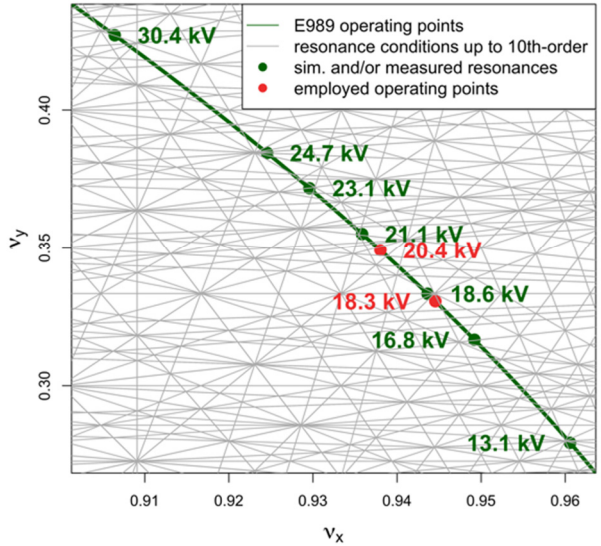

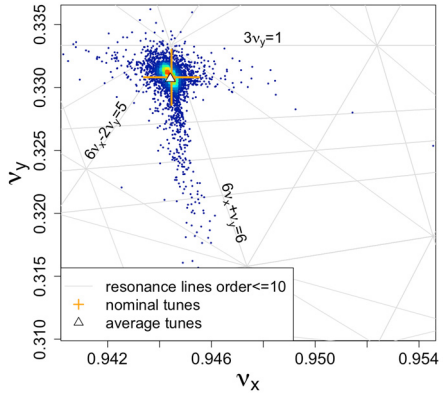

- Geometry of plates introduces nonlinearities.

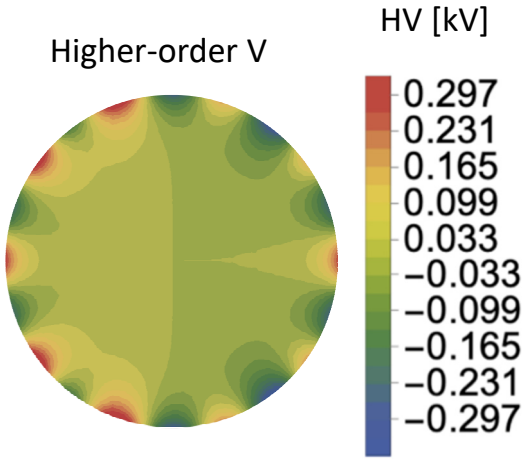

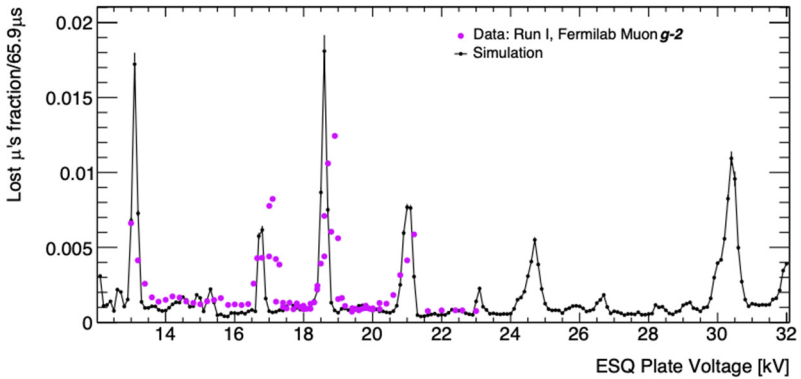

- $3\nu_y = 1$ resonance near operation setpoint. Main driving term from magnetic skew sextupole.
- Beam decoherence ($\tau \approx 190$ μs) driven by electric 20-pole.

Beam dynamics systematic effects

Nonnegligible when:
- Muon collimation changes overall phase (C_{ml}). [-11(5) ppb]
- Muon beam drifts during measurement (C_{pa}). [-158(75) ppb]

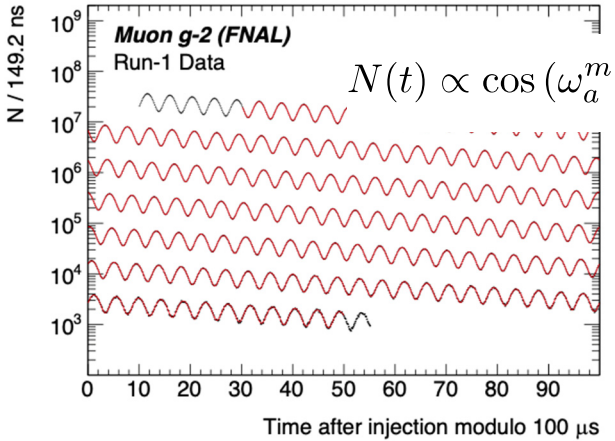

$$N(t) \propto \cos\left(\omega_a^m t + \varphi_0(t)\right) = \cos\left(\omega_a \left[1 + \left\langle \frac{\Delta\omega_a}{\omega_a} \right\rangle + \frac{1}{\omega_a}\frac{d\varphi_0}{dt}\right] t + \varphi_0 + \cdots\right)$$

$$\frac{d\mathbf{S}}{dt} = \boldsymbol{\omega}_s \times \mathbf{S}\,, \quad \boldsymbol{\omega}_s = -\frac{q}{m}\left[\left(a + \frac{1}{\gamma}\right)\mathbf{B} - a\frac{\gamma}{\gamma+1}(\boldsymbol{\beta}\cdot\mathbf{B})\boldsymbol{\beta} - \left(a + \frac{1}{\gamma+1}\right)\frac{\boldsymbol{\beta}\times\mathbf{E}}{c}\right]$$

Nonnegligible when:
- Muon beam has nonzero momentum spread (C_e). [489(53) ppb]
- Muons exhibit vertical oscillations (C_p). [180(13) ppb]

$$\omega_a \approx \omega_a^m \left[1 + C_e + C_p + C_{ml} + C_{pa}\right]$$

E-field correction

Pitch correction

Muon loss correction

Phase-Acceptance correction

*Values in red from Run-1.

Beam dynamics systematic effects: Pitch correction

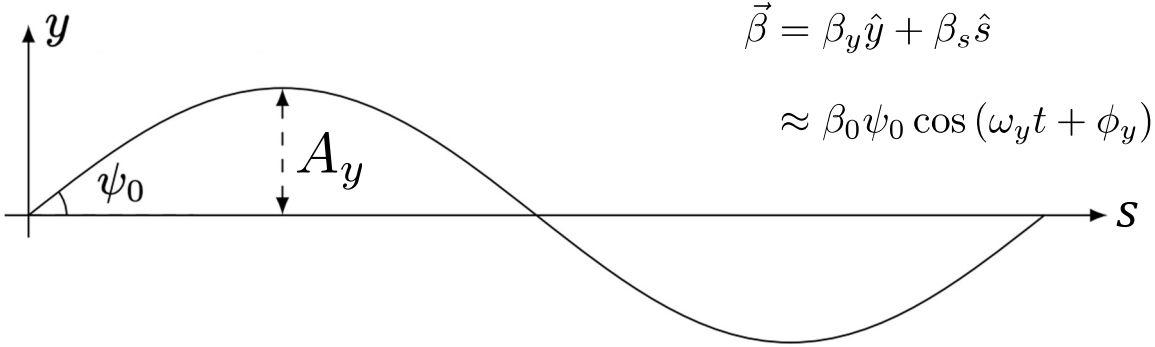

$$\vec{\beta} = \beta_y \hat{y} + \beta_s \hat{s}$$

$$\approx \beta_0 \psi_0 \cos\left(\omega_y t + \phi_y\right) \hat{y} + \beta_0 \left(1 - \frac{\psi_0^2}{2} \cos^2\left(\omega_y t + \phi_y\right)\right) \hat{s}$$

$\omega_a \approx 1.44$ rad/μs, $\omega_y \approx 13.8$ rad/μs

$$C_p = \left\langle \frac{\psi_0^2}{4} \left(1 + \frac{\omega_a^2}{\gamma_0^2 \left(\omega_y^2 - \omega_a^2\right)}\right) \right\rangle$$

$$\approx \frac{\langle \psi_0^2 \rangle}{4} = \frac{\langle y'^2 \rangle}{2} \approx \frac{n}{2\rho_0^2} \langle y^2 \rangle = \frac{n}{4\rho_0^2} \langle A_y^2 \rangle$$

$C_p = 180(13)$ ppb for Run-1

Vertical position

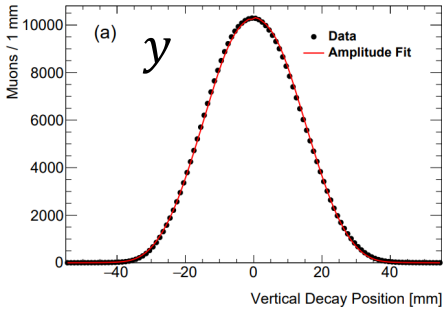

Betatron amplitude

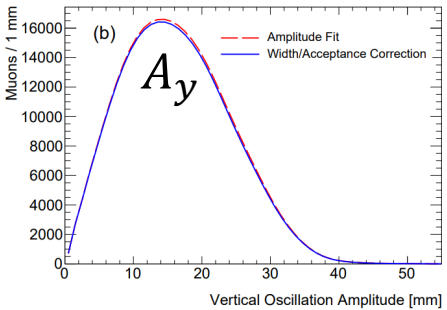

- Systematic errors dominated by tracking reconstruction and quadrupole calibration.

Beam dynamics systematic effects: Muon loss correction

- Bias from phase-momentum correlation and momentum-dependent muon loss:

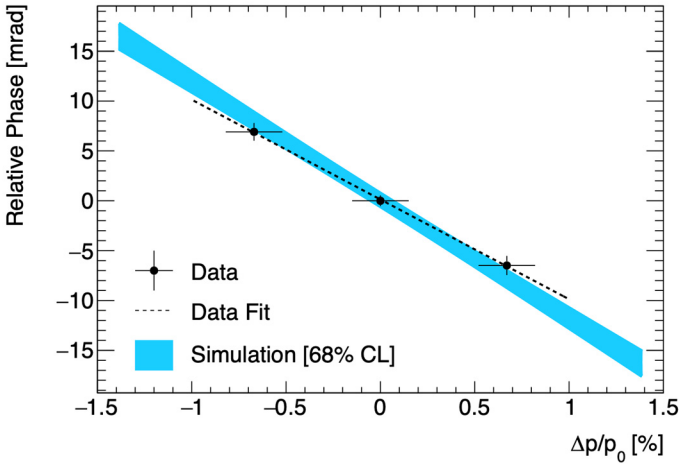

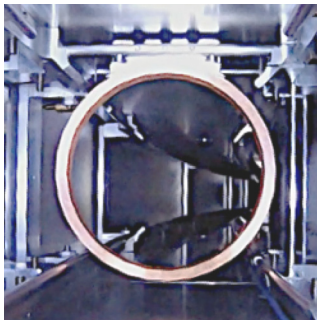

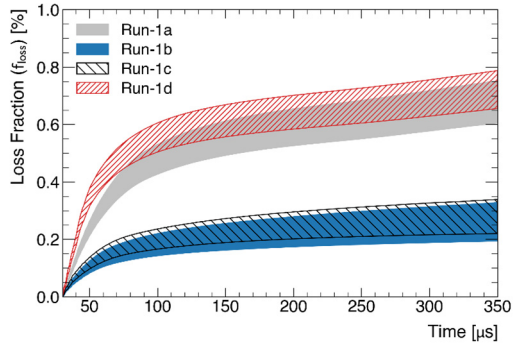

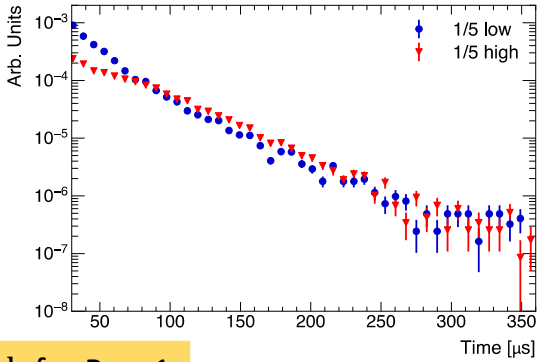

$$\frac{d\varphi_0}{dt} = \frac{d\varphi_0}{d\langle p\rangle}\frac{d\langle p\rangle}{dt}$$

- Muon loss greatly reduced in posterior Runs.

$C_{ml} = -11(5)$ ppb for Run-1

Beam dynamics systematic effects: Phase-Acceptance correction

- Unstable transverse motion of muon beam, detection acceptance, and spatial dependence of phase bias ω_a:

$$\varphi_0^{c_k}(t) = \arctan \frac{\sum_{ij} M_{T,k}(x_i, y_j, t) \cdot \varepsilon_{c,k}(x_i, y_j) \cdot A_k(x_i, y_j) \cdot \sin(\varphi_{0,k}(x_i, y_j))}{\sum_{ij} M_{T,k}(x_i, y_j, t) \cdot \varepsilon_{c,k}(x_i, y_j) \cdot A_k(x_i, y_j) \cdot \cos(\varphi_{0,k}(x_i, y_j))}$$

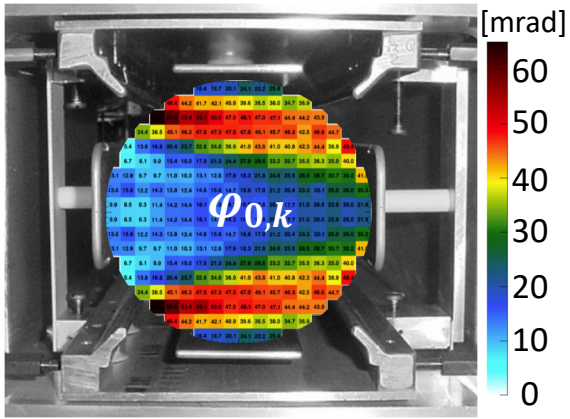

$C_{pa} = -158(75)$ ppb for Run-1

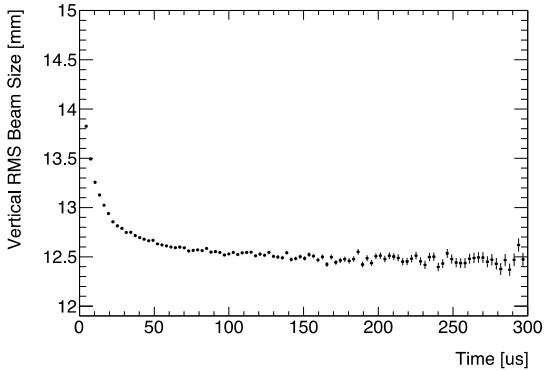

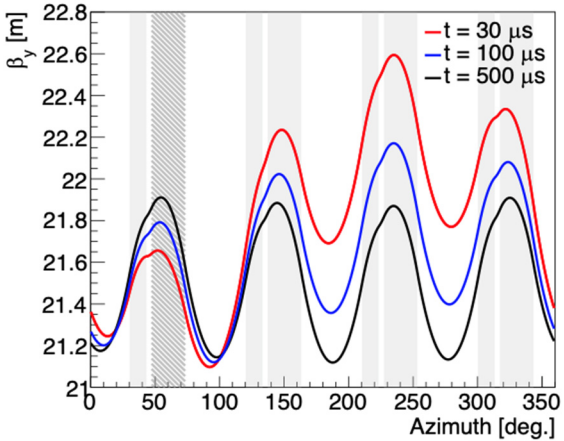

Beam dynamics systematic effects: ω_a and CBO

- Beam betatron motion and detector acceptance introduce additional oscillations in positron histogram.

Physical frequency	Calculated expression	Frequency (rad/μs) $n = 0.108$	$n = 0.120$
ω_c	v/R_0	42.15	42.15
ω_x	$\sqrt{1-n}\omega_c$	39.81	39.54
ω_y	$\sqrt{n}\omega_c$	13.85	14.60
ω_{CBO}	$\omega_c - \omega_x$	2.34	2.61
ω_{VW}	$\omega_c - 2\omega_y$	14.45	12.95
ω_a	$ea_\mu B/m$	1.44	1.44

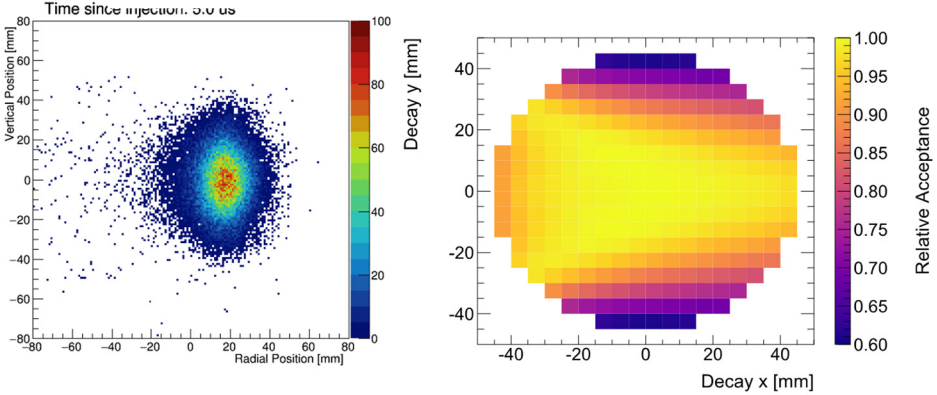

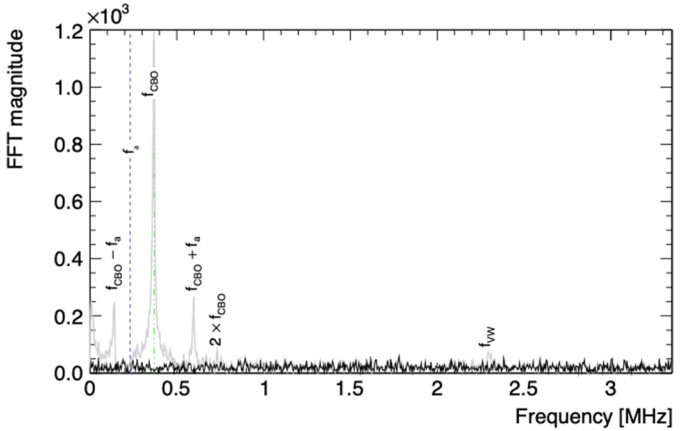

$$F(t) = N_0 \cdot N_x(t) \cdot N_y(t) \cdot \Lambda(t) \cdot e^{-t/\gamma\tau_\mu} \times [1 + A_0 \cdot A_x(t) \cdot \cos(\omega_a(R)t + \phi_0 \cdot \phi_x(t))]$$

$$\begin{aligned}
N_x(t) &= 1 + e^{-1t/\tau_{\mathrm{CBO}}} A_{N,x,1,1} \cos(1\omega_{\mathrm{CBO}} t + \phi_{N,x,1,1}) \\
&\quad + e^{-2t/\tau_{\mathrm{CBO}}} A_{N,x,2,2} \cos(2\omega_{\mathrm{CBO}} t + \phi_{N,x,2,2}), \\
N_y(t) &= 1 + e^{-1t/\tau_y} \quad A_{N,y,1,1} \cos(1\omega_y \quad t + \phi_{N,y,1,1}) \\
&\quad + e^{-2t/\tau_y} \quad A_{N,y,2,2} \cos(1\omega_{\mathrm{VW}}\ t + \phi_{N,y,2,2}), \\
A_x(t) &= 1 + e^{-1t/\tau_{\mathrm{CBO}}} A_{A,x,1,1} \cos(1\omega_{\mathrm{CBO}} t + \phi_{A,x,1,1}), \\
\phi_x(t) &= 1 + e^{-1t/\tau_{\mathrm{CBO}}} A_{\phi,x,1,1} \cos(1\omega_{\mathrm{CBO}}\, t + \phi_{\phi,x,1,1}).
\end{aligned}$$

Conclusion

- A combination of beam preparation, injection, collimation, and storage provides the mean to reach the experiment's precision goal.

- The highly uniform magnetic field and electric focusing system allows for a uniform evolution of the muons' spin precession and cyclotron frequencies.

- Momentum spread and vertical betatron motion introduce additional spin dynamics. Also, detection effects and mechanical muon losses bias the measured anomalous precession frequency.

- With well-established beam dynamics corrections, effects are quantified and applied to the experimental measurements.

TABLE II. Values and uncertainties of the $\mathcal{R}'_\mu$ correction terms in Eq. (4), and uncertainties due to the constants in Eq. (2) for a_μ. Positive C_i increase a_μ and positive B_i decrease a_μ.

Quantity	Correction terms (ppb)	Uncertainty (ppb)
ω_a^m (statistical)	⋯	434
ω_a^m (systematic)	⋯	56
C_e	489	53
C_p	180	13
C_{ml}	−11	5
C_{pa}	−158	75
$f_{\text{calib}}\langle\omega_p(x,y,\phi)\times M(x,y,\phi)\rangle$	⋯	56
B_k	−27	37
B_q	−17	92
$\mu'_p(34.7°)/\mu_e$	⋯	10
m_μ/m_e	⋯	22
$g_e/2$	⋯	0
Total systematic	⋯	157
Total fundamental factors	⋯	25
Totals	544	462

*From Run-1 analysis

THANKS!